Iraqi Journal of Physics, 2018 *Vol.16, No.37, PP. 156-165*

DOI: 10.20723/ijp.16.37.156-165

The effects of silica addition on the structural, electrical and mechanical characteristics of $MgAl_2O_4$ spinel ceramic phase

Muthafar F. Al-Hilli and Nadher I. Mohammed

Department of Physics, College of Science, University of Baghdad, Baghdad, Iraq

E-mail: natheri19990@gmail.com

Abstract

The ceramic compound $Mg_{1-x}Si_xAl_2O_4$ (x= 0, 0.1, 0.2, 0.3, 0.4) was prepared from nano powder of Al_2O_3 and MgO doped with Nano powder of SiO_2 at different molar ratios. The specimens were prepared by standard chemical solid reaction technique and sintered at 1450 ^{o}C. Structure of the specimens was analyzed by using X-ray diffraction (XRD). The X-ray patterns of the specimens showed the formation of pure simple cubic spinel structure $MgAl_2O_4$ phase with space group of $Fd\bar{3}m$. The average grain size and surface topology were studied by atomic force microscopy. The results showed that the average grain size was about 73-90 nm. The DC electrical properties of the specimen were measured. The apparent density was found to increase and the porosity and water absorption were found to decrease with increase of Si addition. Mechanical properties were characterized by Vicker's micro hardness and Brazilian fracture test to measure the fracture toughness of the samples. The micro hardness decreased with Si addition increase. Fracture toughness increased with the increase in Si addition.

Key words

Structure, ceramics, porous structure, electrical, $MgAl_2O_4$.

Article info.

Received: Oct. 2017
Accepted: Jan. 2018
Published: Jun. 2018

دراسة تاثيرات اضافه السليكا بتراكيز مختلفة على الخصائص التركيبية الكهربائية والميكانيكية لطور السبينل السيراميكي $MgAl_2O_4$

مظفر فؤاد جميل الحلي و نذير أبراهيم محمد

قسم الفيزياء، كلية العلوم، جامعة بغداد، بغداد، العراق

الخلاصة

تم تصنيع المركب السيراميكي $Mg_{1-x}Si_xAl_2O_4$ عن طريق خلط مساحيق نانوية من اوكسيد الالمنيوم / اوكسيد المغنيسيوم وتم تطعيمه باضافة اوكسيد السليكا بنسب مختلفة. تم تحضير العينات بطريقة كبس المساحيق وبدرجه حراره تلبيد مقدارها 1450 درجه مئوية. تم تحليل التركيب البنيوي بواسطه جهاز فحص حيود الأشعة XRD وقد تبين ان جميع العينات تملك تركيب نقي مكون من المكعب البسيط الذي ينتمي الى المجموعه الفضائية $Fd\bar{3}m$. تم دراسة التركيب المجهري للنماذج بواسطه جهاز المايكروسكوب ذو القوة الذرية AFM. ولقد ظهر ان معدل الحجم الحبيبي يتراوح بين 73-90 نانومتر. درست الخصائص الكهربائية تحت التيار المستمر. لقد وجد ان الكثافة الظاهرية تزداد والمسامية والامتصاصية المائية تقل تبعا الى زياده نسبه اضافه السيلكا. لقد تم دراسه الخصائص الميكانيكيه للنموذج السيراميكي النقي والمطعم بالسيلكا عن طريق فحص الصلاده المايكرويه والقابليه التحمليه للانضغاط القطري حيث وجد ان الصلاده تنخفض مع زيادة نسبة اضافة السليكا بينما متانة الكسر تزداد مع زيادة نسبة الاضافة.

Introduction

Nano structured magnesium aluminate ($MgAl_2O_4$) spinel is one of the most interesting refractory oxides of vast technological importance as a structural ceramic material. It possesses useful physical, chemical and thermal properties, both at ambient and elevated temperatures [1, 2]. Also it possesses high hardness, strength, and chemical resistance, and therefore it has potential applications as armor [3]. The bonding type in $MgAl_2O_4$ is ionic, which makes this material classified as an insulator. Not long ago $MgAl_2O_4$ has received more attention as a dielectric material. The mechanism of polarization in spinel aluminates is governed by the arrangement of ions in different sites [4]. Synthesizing and preparation of spinel $MgAl_2O_4$ is known since long. A numerous techniques such as conventional solid-state-reaction, sol-gel, and spray drying and organic gel-assisted citrate complication were widely utilized [5].

In this study, a series of magnesium aluminate ($MgAl_2O_4$) doped with silica at different molar ratios was obtained. In this context, the substitution of Si at Mg site in $MgAl_2O_4$ and its possibility of tailoring the structure of the resultant compound and therefore improving the mechanical and electrical properties which could further widen its range of applications were investigated.

Experimental

Single phase specimen of pure and SiO_2 doped $MgAl_2O_4$ having general formula as $Mg_{1-x}Si_xAl_2O_4$ (x= 0, 0.1, 0.2, 0.3, 0.4) were prepared by using standard chemical solid reaction technique. The analytical grade starting reagents employed were magnesium oxide MgO, Aluminum oxide Al_2O_3 silicate dioxide SiO_2 as given in Table 1. The precise amounts of the reagents were mixed in the proper molar ratios. The powders were mixed for about 5min by using a speed mixer with the maximum speed of 2000 rpm. The powder were pressed by using hydraulic press with pressure of 10 ton to produce pellets with diameter of 15 mm the specimen were sintered at temperature of 1450 °C and soaking time of 2h.

Table 1: The source, particle size and purity of raw material oxides.

oxide	Particle size (nm)	Purity and Manufacture Company
MgO	30 -40	99.9% ISO9001 (Qing Chong, china)
Al_2O_3	20 -30	99.0% (Griffin &George LTD, London, England)
SiO_2	20 -30	99.5% (Griffin &George LTD, London, England)

The porosity, apparent density and water absorption were calculation for all sintered specimens using Archimedes' principle according to the standard specifications [ASTM C373 test methods] [6, 7]. As follows:-

1- The specimens were weighed using a digital balance of accuracy 10^{-4} g after it were dried at 120 °C for two hours using an oven and taking the weight of dry specimen (D).

2- Specimens submerged in boiling water for five hours and left in the water for 24 hours and then taking the immersed weight (I).

3- Specimens were taken out of the water and wiped with a wet piece of tissue and was weighed once again to find the soaked weight S. Apparent porosity, water absorption and apparent density were calculated using the following equations (S)

Apparent porosity $$AP = \frac{S-D}{S-I} * 100\% \quad (1)$$

Water absorption $$\%W.A = \frac{S-D}{D} * 100\% \quad (2)$$

Apparent solid density $$\rho = \frac{D}{D-I} \quad (3)$$

X-ray diffraction (XRD) analysis was performed using automated Philips type PW 1840 diffractometer equipment with Cu Kα radiation source (20 mA/30 kV). The specimens were scanned in the 2θ range between 20-80^o (at scan rate 2θ = 3^o /min). AFM was performed by using AA3000 scanning probe Microscopy by Angstrom Advanced Inc. (USA). The electrical resistivity was measured as a function of temperature over the range 290-430 K. The measurements were done using sensitive digital electrometer type Keithley 616 and electrical oven. Hall Effect measurements were done by Van der pauw (Ecopia HMS-3000) which were carried out at room temperature using the four probe technique. The principle of Hall effect refers to potential difference (Hall voltage) on opposite sides of a thin sheet of conducting or semi-conducting material through which an electric current is flowing, created by a magnetic field B=0.55 Tesla were determined using LCR meter bridge. For this purpose silver paste was applied on both sides of the specimen to make sure of good Ohmic contacts. The Hall-effect measurements involved measuring the Hall coefficient (R_H), Hall mobility (μ_H) and sheet carrier concentration (n_H). The measurement of AC-electrical conductivity ($\sigma_{a.c}$), and its variation with frequency was carried out using LRC meter IA (impedance analyzer) (4274 A HEWLETT PACKARD) over the frequency range (10 kHz-1 MHz). The mechanical properties were characterized by micro hardness (H_V) and disk fracture test (Brazilian disk fracture) (σ_f).

Results and discussion

Fig.1. shows XRD patterns of specimen with different doping of Si^{+2} ions. The characteristic peaks belong to the (Fd3m) cubic spinel space group. It indicates the formation of the single spinel phase structure. A crystalline secondary phase was identified as garnet ($MgSiAl_2O_4$) in a small amount existed**.** Magnesium aluminate ($MgAl_2O_4$) because of its high melting point and chemical stability, shows remarkable electrical, magnetic and other physical characteristics.

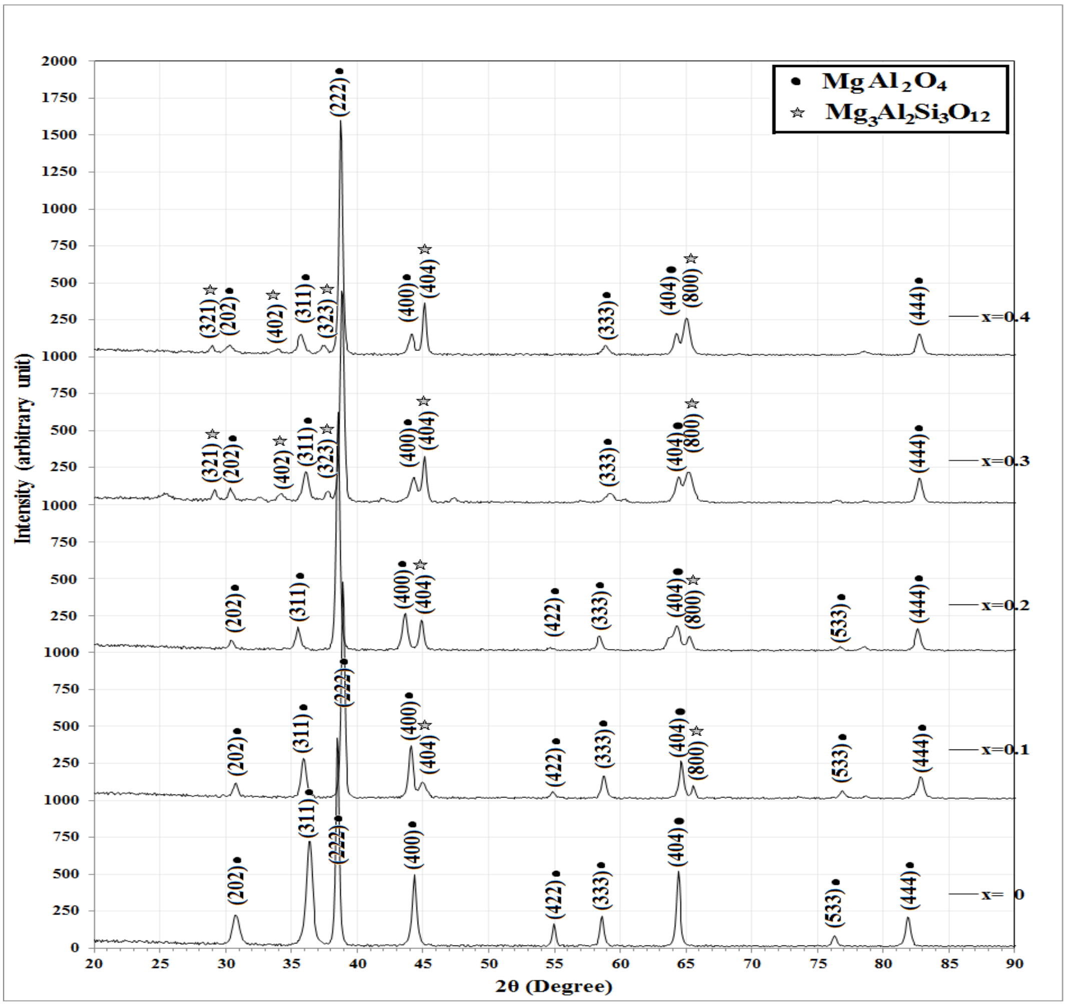

Fig.1: XRD patterns of ($Mg_{1-x}Si_xAl_2O_4$) where x= 0, 0.1, 0.2, 0.3, 0.4.

Most of the spinel compounds have the space group Fd3m. The spinel structure AB_2O_4 consists of almost closely packed oxygen anions, in which the tetrahedral and octahedral sites are occupied by cations. The unit cell may be obtained by doubling this fcc oxygen sub-lattice, along each of three directions. If the cations A and B are occupied at the '8' tetrahedral 'A' sites, and 16 octahedral 'B' sites, out of the 64 and 32 available sites, the arrangement is called the stoichiometric or normal spinel. In the normal spinel, Mg^{2+} ions occupy the tetrahedral positions, and Al^{3+} ions occupy octahedral positions. There are some spinel's systems which are occupied by both trivalent the tetrahedral positions and divalent ions known as the inverse spinel structure [8]. It may be due to the arrangement of metal ions in different A and B sites while the composition changes. X-ray diffraction shows that all the specimens are of $MgAl_2O_4$ single phase. The lattice parameter (a) was determined experimentally from the d_{hkl} spacing using the following equation for cubic structure Eq. (4) [9]. The peak with the Miller indices (311) was used in the X-ray measurement shown in Table 2. The ionic radii of tetrahedral A-sites in the spinel structure (r_A) and B- octahedral (r_B) can be determined from the Eqs. (5, 6), where r_A is the tetrahedral A-sites radii, r_B is octahedral B-sites radii and u is the oxygen parameter. The ideal u value is close to 0.375 (Å) in spinel, and r (O^{-2}) is the ionic radii of oxygen.

$a = d_{hkl}\ (h^2+k^2+l^2)^{1/2}$ (4)

$r_A = (u-1/4)\ a\ (3)^{1/2} - r\ (O^{2-})$ (5)

$r_B = (5/8 - u)\ a - r\ (O^{2-)}$ (6)

where the R_B and R_A is ionic destines bond, and (h k l) are the miller indices [10].

Table 2: Lattice parameter A- and B- site radii, bond length and oxygen parameter as a function of Si content.

Si content	**a (Å)**	**d (Å)**	**Crystallite size (nm)**	**r_A (Å)**	**r_B (Å)**	**R_A (Å)**	**R_B (Å)**	**(h k l)**
0	8.1870	2.4685	16.2	0.39256	0.666752	7.090266	1.771768	(3 1 1)
0.1	8.2806	2.4967	20.7025	0.4128	0.69015	7.171248	1.792005	(3 1 1)
0.2	8.3808	2.5269	19.1754	0.43449	0.7152	7.258024	1.813689	(3 1 1)
0.3	8.2464	2.4864	16.9145	0.4054	0.6816	7.14163	1.784603	(3 1 1)
0.4	8.3267	2.5106	15.9486	0.42278	0.7016	7.211172	1.801981	(3 1 1)

The qualitative results showed that the phases in calcined spinel specimen at temperatures 1450 °C consisting of only $MgAl_2O_4$ spinel phase having crystallite size below 25 nm.

Fig. 2 shows the AFM images for specimens $MgAl_2O_4$ doped with Si where x=0, x=0.1 and x=0.4. AFM images showed that all specimens have granular nature. The average grain size and average roughness as determined from AFM are given in Table 3. Both grain size and surface roughness increased with the increase of substitution which refers to the increases in the strength of bond of linking atoms, where the average grain size of x=0.1 and x=0.4 were 94.89 nm and 90.22 nm, respectively, as shown in Table 3. On the other hand the average roughness decreases from 6.65 nm to 4.33 nm for x=0.1 and 0.4, respectively.

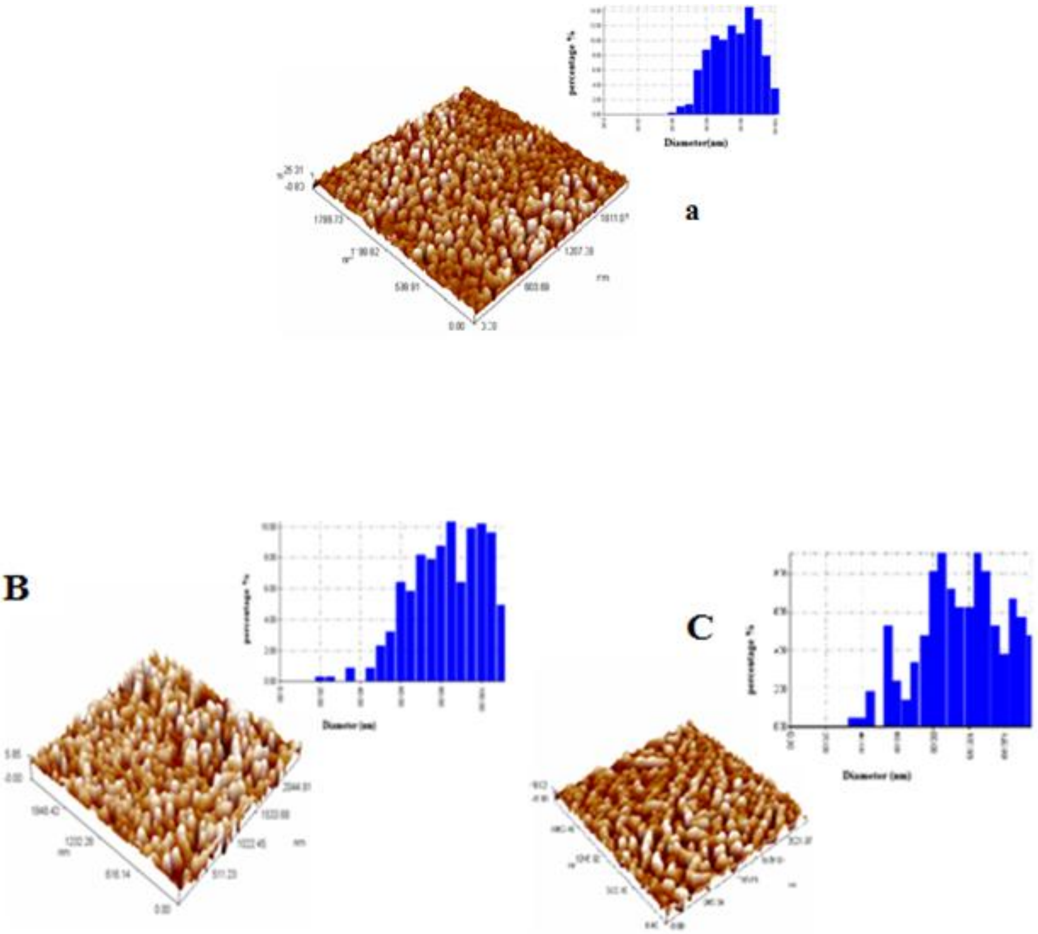

Fig. 2: AFM graphs of ($Mg_{1-x}Si_xAl_2O_4$) where (a) x= 0, (b) x=0.1 and (c) x=0.4

Table 3: Average grain size and average roughness obtained from AFM measurements for ($Mg_{1-x}Si_xAl_2O_4$) where x= 0, 0.1, 0.4.

X %	Grain Size(nm)	Average Roughness.(nm)
0	73.93	4.38
0.1	94.89	6.65
0.4	90.22	4.33

Figs. 3, 4 and 5 show the results of apparent density, apparent porosity and water absorption as a function of SiO_2 content respectively. Apparent density was found to decrease with SiO_2 content. This decrease corresponds to the mixing rule; the reason behind the decrease in apparent density is the increase of the apparent porosity exists inside the structure.

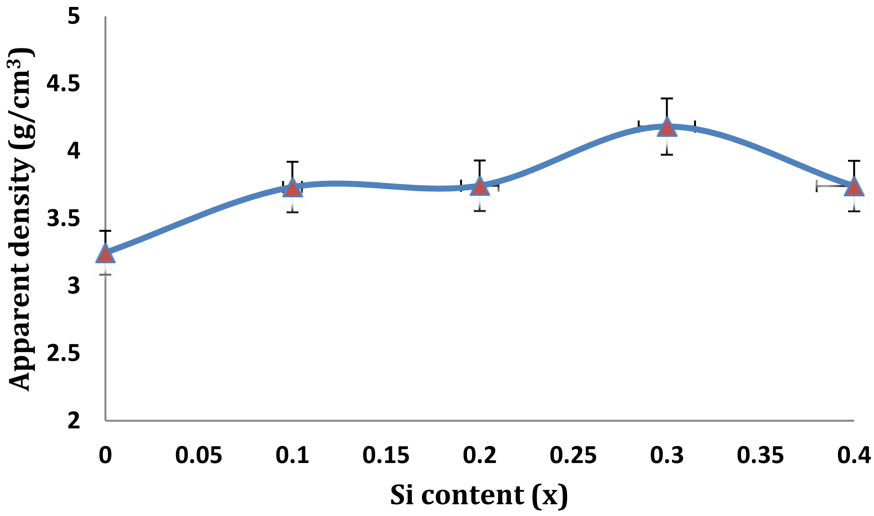

Fig. 3: The density of ($Mg_{1-x}Si_xAl_2O_4$) where x= 0, 0.1, 0.2, 0.3, 0.4.

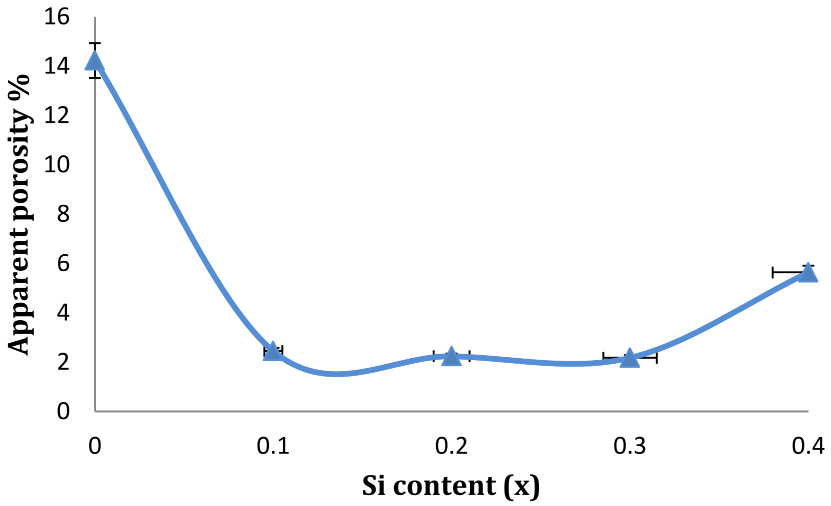

Fig. 4: The apparent porosity of ($Mg_{1-x}Si_xAl_2O_4$) where x=0, 0.1, 0.2, 0.3, 0.4.

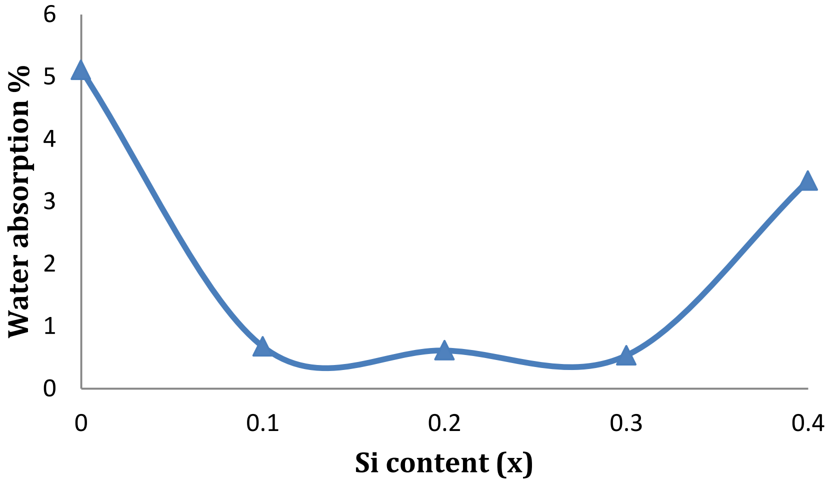

Fig. 5: The Water Absorption of $Mg_{1-x}Si_xAl_2O_4$ where x= 0, 0.1, 0.2, 0.3, 0.4.

Fig. 6 shows the electrical resistivity against temperature of $MgAl_2O_4$ sample doped with different ratios of Si ions. The decrease in electrical resistivity with temperature indicates the semiconducting nature of the $MgAl_2O_4$ compound. The temperature dependence of electrical resistivity arises because of the drift mobility of electrical charge carriers rather than by the localized charge carriers [11]. The low values of resistivity may be attributed to the small crystalline size, as shown in increased [12]. Table 3. In general, the conduction mechanism in semiconductors is greatly influenced by inter-crystalline grain boundaries and strain fields associated with dislocation network. This behavior may be explained from the temperature dependent electrical resistivity of the samples surface. There is an electron across the energy transition from the filled valence-band level to the unfilled conduction –band states. The electrical resistivity of samples increased as the content of Si.

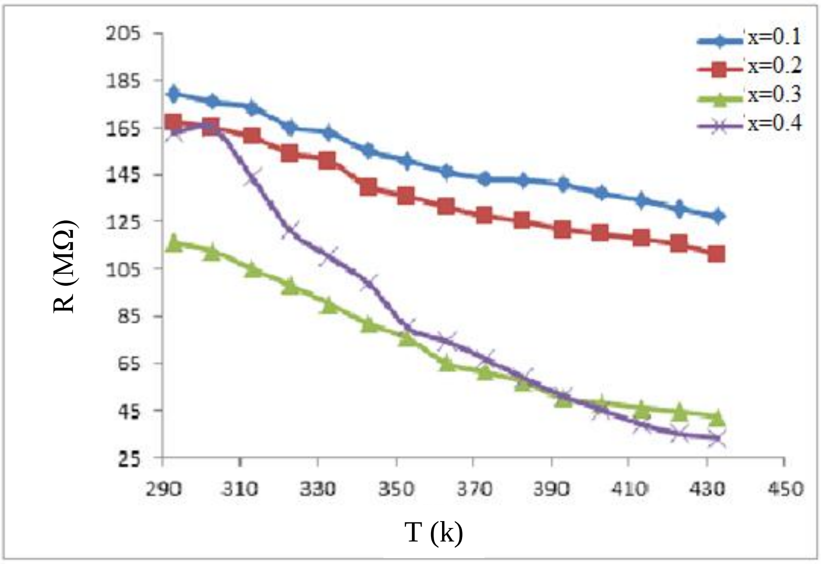

Fig. 6: The change of resistance with temperature for $Mg_{1-x}Si_xAl_2O_4$ where x= 0.1, 0.2, 0.3, 0.4.

The results of activation energies Ea_1, Ea_2 are shown in Table 4. It may be noticed that there are two transport mechanisms, giving rise to two activation energies Ea_1 and Ea_2. At higher temperature range (373-443 k), the conduction mechanism is due to carrier excited into the extended states beyond the mobility edge. At lower temperature range (293-373 k) the conduction mechanism is due to carries excited into localized states at the edge of the band.

Table 4: Shows the activation energy of $Mg_{1-x}Si_xAl_2O_4$ where x= 0, 0.1, 0.2, 0.3, 0.4.

specimen	E_{a1}	E_{a2}
X=0	-0.1268	-0.0705
X=0.1	-0.1462	-0.1373
X=0.2	-0.0117	-0.0838
X=0.3	-0.1099	-0.0304
X=0.4	-0.0296	-0.0902

Fig.7 shows that the microhardness decreased with Si addition due to the high porosity. In general the hardness of $Mg_{1-x}Si_xAl_2O_4$ is still high and within the acceptable limits. Results of the diametrical compression strength obtained from the Brazilian test (σ_f) is shown in Fig. 8. The diametrical compression increased with Si addition. This could be attributed to the increase in density since the compression strength varies proportionally with the density.

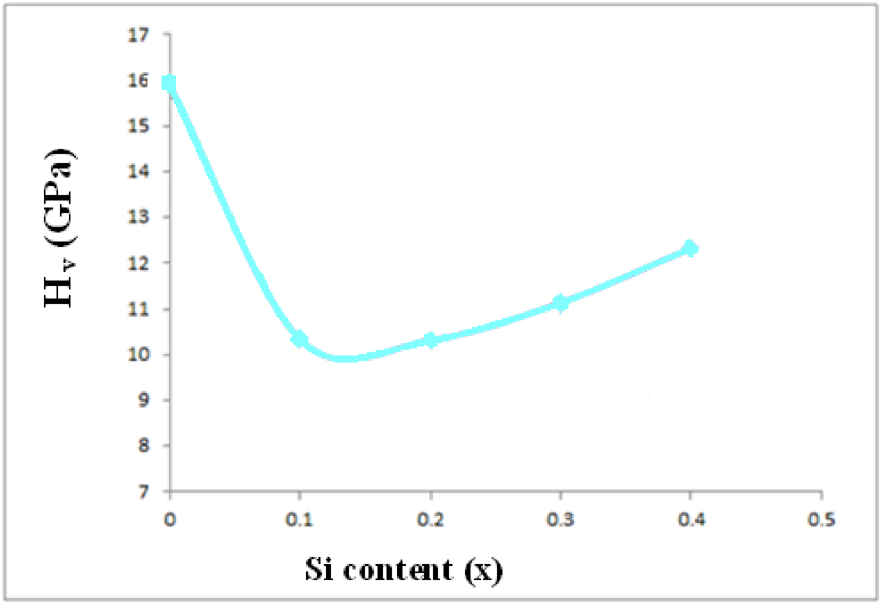

Fig. 7: Shows the micro hardness (Vickers hardness) of $Mg_{1-x}Si_xAl_2O_4$ where x= 0, 0.1, 0.2, 0.3, 0.4.

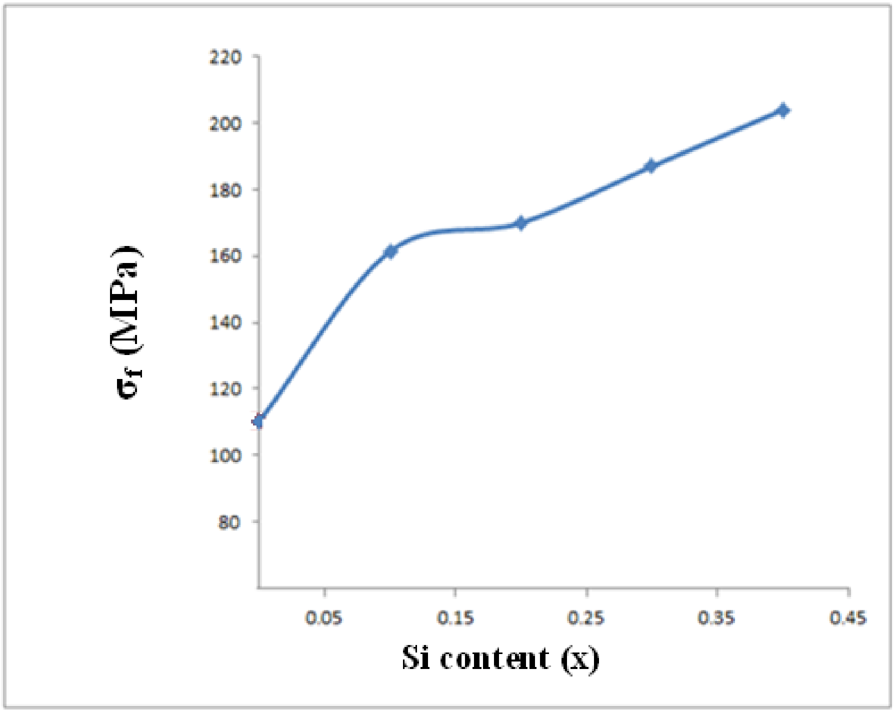

Fig. 8: A plot diametrical compression (σ_f) against Si addition % of $Mg_{1-x}Si_xAl_2O_4$ where x= 0, 0.1, 0.2, 0.3, 0.4.

Conclusions

X-ray spectra for specimens indicated the formation of crystalline cubic spinel structure phase ceramic with the appearance of small amount of secondary phases. The average grain size for pure specimen is less than the average grain size of doped specimen. The result of Hall coefficient showed an n-type semiconductor behavior. The conduction mechanism in this ceramic is due to hopping of electron between Mg^{+2} and Al^{3+}. The mechanical properties showed good results for Si doping.

References

[1] Lim Rooi Ping, Abdul-Majeed Azad, Teng Wan Dung, Materials Research Bulletin 36 (2001) 1417-1430.

[2] H.I. Klym, I.V. Hadzaman, Proceedings of the International Conference Nanomaterials: Applications and Properties, 2, 4 (2013) 22-1_22-2.

[3] V.T. Gritsyna, Yu.G. Kazarinov, A.O. Moskvitin, I.E. Reimanis, Acta Physica Polonica A, 117, 1 (2010) 161-165.

[4] Rohan Samkaria, Vimal Sharma, International Journal of Modern Physics: Conference Series, 22 (2013) 361-364.

[5] U. Önen and T. Boyraz, Acta Physica Polonica, A 125, 2 (2014) 488-490.

[6] W. Ryan, and C. Radford, pergamon press, UK, 1987.

[7] ASTM annual book of standards, vol. (15.01), (C-1025), 1985.

[8] G. Martin, "Encyclopedia of composite materials and components" John Wiley and Sons. pp. 588, 1983.

[9] K.J. Standely, Oxide Magnetic Materials, 2nd edition, Clarendon press, oxford, 1972.

[10] Muthafar F. Al-Hilli, Journal of Magnetism and Magnetic Materials, 324 (2012) 873-879.

[11] M. Din, F. Ahmad, I. Ahmad, M. Farid, M. T. Iqbal, M. A. Murtaza, G. Akhtar, M. N. Shakir, I. Warsi, M. F., M. A. Khan, J. Alloy Compound, 584 (2014) 646-651.

[12] D. Ravinder and P. V. B. Reddy, Mater. Lett., 57(26-27) (2003) 4344-4350.